Performance of Proton Exchange Membrane Fuel Cell at High-Altitude Conditions

Joseph W. Pratt,* Jacob Brouwer,† and G. Scott Samuelsen‡
National Fuel Cell Research Center, University of California Irvine, Irvine, California, 92697-3550

The effects of oxygen concentration and ambient pressure on fuel cell performance are explored both in theory and in experiment. For fuel cells in general the effect due to a change in oxygen concentration is shown to be fundamentally different than the effect due to a change in cathode pressure, even if partial pressure is held constant. For a proton exchange membrane fuel cell, a significant reason for this difference comes from the nature of mass diffusion processes in the fuel cell structure, which infers that there is an optimum fuel cell design (macroscale and microscale) for a given operating pressure and oxygen concentration. In the experimental work a proton exchange membrane fuel cell was subjected to varying atmospheric conditions from sea level to 53,500 ft (16,307 m) with results analyzed up to 35,000 ft (10,668 m). The results showed that at low current density operation a decrease in either cathode pressure or concentration led to an increase in irreversible losses associated with reaction kinetics (activation polarization) and confirmed the differing effects of cathode pressure and oxygen concentration. Consideration of all these effects enables both fuel cell- and system-level optimization of aeronautical fuel cell-based power systems.

Nomenclature

A_{cell}	=	area of a single cell, cm^2
F	=	Faraday's constant, $96,485$ C/mol
i	=	current density, mA/cm^2
i_L	=	limiting current density, mA/cm^2
i_o	=	exchange current density, mA/cm^2
n	=	number of moles of electrons produced per mole of reactant reacted
P	=	pressure, kPa absolute
P_A	=	anode pressure, kPa absolute
P_C	=	cathode pressure, kPa absolute
P_T	=	total pressure, kPa absolute
pY	=	partial pressure of species Y, kPa absolute
R	=	universal gas constant, 8.314 kJ/kmol $\cdot$ K
R_{cell}	=	bulk area specific resistance of a cell, $k\Omega \cdot cm^2$
T	=	temperature, K
V	=	voltage, V
V_{Oper}	=	operating voltage, V
xY	=	concentration of species Y
xY, exit	=	concentration of species Y at fuel cell exit
xY, inlet	=	concentration of species Y at fuel cell inlet
y	=	reaction order
α	=	charge transfer coefficient (empirical)
λ	=	stoichiometric ratio for air

Introduction and Background

FUEL cells are continuing to gain credibility as alternative power sources in many applications, including stationary power, automotive propulsion, auxiliary power for large trucks, remote or backup power for telecommunications and other sensitive equipment, and even portable power for personal electronic devices. And although fuel cells have been used in space applications for decades, recently the aerospace industry has increased its attention on the possibility of using fuel cells in other applications, such as commercial aircraft auxiliary power units (APUs) [1,2], propulsive and/or auxiliary power for high-altitude long endurance (HALE) aircraft and orbiting platforms [3,4], and unmanned aerial vehicles (UAVs) [5,6].

Analysis of the feasibility of using fuel cells in these applications demands accurate understanding and predictions of fuel cell behavior at the conditions encountered in the flight scenarios of each application. For example, a passive fuel cell operating on an aircraft at 35,000 ft (10,668 m) will need to produce power using air at a pressure that is only one-quarter of sea level pressure, and withstand temperatures of $-55°C$ or lower. These are severe conditions for fuel cells and the published experimental data for these operating conditions are limited.

In practice, subatmospheric pressure operation of a fuel cell is usually avoided through the use of compressed air and fuel. Or in the case of unpressurized fuel cell operation at high altitudes, the realized voltage and efficiency loss is characterized by a "derate" factor; for example, one manufacturer states that above 1000 ft (305 m) in altitude total power output decreases by 1.5% per 1000 ft (305 m) [7]. However, the value of a particular derate factor used to predict performance in terrestrial low-pressure conditions [altitudes less than 10,000 ft (3,048 m)] may be different than that used to predict performance in the ranges of aircraft flight [altitudes between 20,000 ft (6,096 m) and 45,000 ft (13,716 m)] and HALE missions [>50,000 ft (15,240 m)]. High-altitude studies are needed to verify or find the correct relationships.

Understanding the impacts of high altitude on fuel cell performance and publishing data obtained from fuel cells operated at high-altitude conditions is important because high-altitude conditions affect fuel cell performance through a complex set of physical, chemical, and electrochemical processes. These processes are typically summarized by accounting for theoretical (Nernst) potential and three types of cell polarization (activation, ohmic, and concentration), each of which may be affected by high-altitude operating conditions. Accurate understanding of the affects of high-altitude conditions on both the fuel cell potential and the polarizations is required for design of aerospace fuel cell systems. Whereas the fuel cell community understands and agrees that fuel cell performance is degraded at high altitude, no data have been published for use in determining the impacts of high altitude on

---

*Graduate Research Assistant, Mechanical and Aerospace Engineering Department. Student Member AIAA.
†Adjunct Assistant Professor, Mechanical and Aerospace Engineering Department.
‡Professor, Mechanical and Aerospace Engineering Department.

proton exchange membrane (PEM) fuel cell performance and there is some controversy regarding the means by which degraded performance is achieved.

When keeping the concentration of oxygen in the reactant stream constant (e.g., using atmospheric air between sea level and 262,000 ft (80,000 m) [8]), the main effect of reduced total pressure operation is a decrease in performance. At a given voltage, the fuel cell will produce less power, or, at a given power setting the irreversible losses increase, reducing voltage and efficiency. This well-known effect has been documented in various texts [9–11], and has been shown in several experiments that demonstrate the opposite effect: increasing total pressure increases performance [12–19] and many experiments have similarly shown that decreasing the concentration of oxygen while keeping the total pressure constant decreases performance [12–23].

Both total pressure and concentration of oxygen affect the partial pressure of oxygen via the simple equation [24]:

$$pO_2 = xO_2 P_T \qquad (1)$$

Therefore a decrease in either concentration or total pressure will decrease the partial pressure. With the appearance of partial pressure in a commonly used form of the Nernst equation [9,10]

$$E = E° + \frac{RT}{nF} \ell n \frac{pH_2(pO_2)^{\frac{1}{2}}}{pH_2O} \qquad (2)$$

it is tempting for many to think of partial pressure as being responsible for changes in performance without considering whether concentration or total pressure (or both) is actually what causes changes in partial pressure. For example, at a total pressure of 1 atm and concentration $xO_2 = 1.0$, the partial pressure pO_2 will be 1 atm. The partial pressure pO_2 will also be 1 atm at a total pressure of 4.8 atm and a concentration $xO_2 = 0.21$ (air). It has been shown, in this case, that a fuel cell behaves differently depending upon which condition is used. Specifically, at low current densities (current density less than the point where the V–i curve begins to deviate from linearity due to mass transport limitations) the fuel cell performed better in the higher total pressure case than in the higher concentration case [17]. Other experiments show the same thing: strictly speaking, it is not partial pressure that affects fuel cell performance, it is concentration and total pressure, and these two variables affect performance in different ways [13,15,16,18].

However, although Ticianelli et al. [14] support this general conclusion, these authors present superior performance for the high-concentration case for all current densities. Thus, there remains some controversy in the literature regarding the impacts of low total pressure on the theoretical potential of a PEM fuel cell. Also, unless proper context is clearly given, it is misleading and technically incorrect to use variations in partial pressure to substitute for variations in concentration or total pressure to determine impacts on fuel cell performance.

Although fuel cells have been operated at altitudes of over 5000 ft (1524 m) for the U.S. Department of Defense's Fuel Cell Demonstration Program [25], and at approximately 6650 ft (2027 m) at Yellowstone National Park [26], the low-pressure operating characteristics of these demonstration projects was secondary. Only a few studies have reported operation of fuel cells at high altitudes with the specific intent of quantifying the effect of low pressure on performance. For example, Cessna and Boeing tested a 1.2 kW-rated Ballard Nexa proton exchange membrane fuel cell (PEMFC) system at pressure altitudes up to 5000 ft (1524 m) and showed a net power decrease to 970 from 1300 W at sea level [27]. Another Ballard system was tested by the U.S. Environmental Protection Agency in Mexico City, Mexico [7400 ft (2256 m)]. This PEMFC power plant (of Ballard's Phase 2 fuel cell bus) was composed of 20 13 kW stacks, and it was shown that at an array voltage of 500 V, string current decreased by 24% from sea level operation [28]. In both of these cases the air supply system was identified as a probable cause of the power loss.

In addition, none of these previous studies were conducted at altitudes useful for most aeronautical applications. The lack of published high-altitude fuel cell performance data is a problem that could misleadingly force aerospace fuel cell designers to only consider expensive and inefficient air pressurization as a means of achieving reasonable high-altitude performance. Alternately, designers could try to extrapolate high total pressure experiments to determine fuel cell performance under low total pressure conditions, or to use low "partial pressure" data (conducted by varying concentration) as a substitute for low total pressure data. The first approach adds equipment (volume, weight, cost, complexity) to a high-altitude fuel cell system, which may be unnecessary. The second approach may not yield accurate results when linearly extrapolated to high altitudes, and the third approach is erroneous.

Unfortunately for the aeronautical community, this implies that experimental results for the operation of fuel cells "at low partial pressures" (by lowering oxygen concentration) cannot be used to predict the affects of total pressure on fuel cell performance at altitude. Note that the experiments referenced in preceding paragraphs all used 1 atm as the lower limit of total pressure. Furthermore, the measured performance of a fuel cell is not only governed by impacts of total pressure on the Nernst potential, but may also be limited by changes in cell polarizations caused by changes in total pressure.

The current work has been accomplished, therefore, to clarify the impacts of altitude on the performance of a PEM fuel cell, provide PEM fuel cell data obtained for aerospace relevant high-altitude conditions, and to elucidate the mechanisms that contribute to the observed high-altitude performance. The objectives of this work are to 1) acquire and publish a set of PEM fuel cell performance data for high-altitude operating conditions, 2) determine the suitability of the voltage potential and polarization theory commonly used to describe performance of atmospheric and pressurized fuel cells for describing the performance of subatmospheric pressure fuel cells (pressure below 1 atm), and 3) discuss implications of the theory and observations for design of aerospace fuel cell systems.

Experiment

The fuel cell used in the present experiment was an annular-type proton exchange membrane fuel cell from DCH Enable Fuel Cell Corp. The air side (cathode) of this fuel cell is passive (there is no mechanical fan or blower conveying air to or away from the cathode). The hydrogen side (anode) is dead-ended, meaning all the hydrogen entering the anode compartment is either consumed by the fuel cell reaction, or wasted due to leakage and crossover. There are 23 cells in series, and the cell active area is approximately 13 cm^2. A detailed description of this kind of PEMFC can be found in [29].

The fuel cell was placed in a vacuum chamber capable achieving pressures of at least 27.8 in Hg vacuum [an absolute pressure of 7.2 kPa (1.05 psia)]. Continuous flow vacuum pumps maintained an airflow through the vacuum chamber at a rate dictated by the experiment run and monitored by a mass flow meter. Air was cooled to the required inlet temperature using cold boil-off gas from a liquid nitrogen dewar via manual control through flat-plate heat exchanger. The relative humidity of the inlet air was manually controlled using a desiccant dryer system upstream of the heat exchanger, and measured at room temperature using a humidity sensor. The reading was converted to a relative humidity measurement at the chamber air inlet temperature using standard water/ice vapor pressure formulations [30,31].

The chamber itself was located in ambient conditions and insulated to thermally isolate it from its surroundings. It was expected that the cold air going into the fuel cell would cause the inside of the chamber to be at a lower temperature than the ambient conditions; however, it became quickly apparent as experiments were conducted that the airflow was not sufficiently high enough to offset the thermal energy generated by the fuel cell. This inevitably led to the inside of the chamber becoming warmer than the ambient temperature, and predicted the insignificance of the air inlet temperature in this experiment (verified later).

Table 1   Instruments used and their and associated uncertainties

	Mass flow meter (Omega FMA1714)	Mass flow meter (Sierra 822)	Thermocouples (generic K-type)	Pressure transducer (Ashcroft K1)	Pressure transducer (Ashcroft K1)	Humidity sensor (Vaisala HMP231)	Current transducer (CR Magnetics CR5210)	Voltage sample (direct)
Use	H_2 flow rate	Airflow rate	Air and stack temperature	Chamber pressure	H_2 inlet pressure	Inlet water content	Fuel cell load current	Fuel cell load voltage
Maximum error (+/−) (includes DAQ hadware)	0.016 SLPM	0.4 SLPM	2°C	1.1 kPa	3.5 kPa	1% reading +0.05% RH	22 mA	5 mV

Table 2   Controlled variables and designed ranges in the experiment

	Pressure, kPa (absolute)	External resistance, Ω	Relative humidity, %	Airflow, SLPM	Air temp., °C
Low	10	15	15	1.0	−60.0
High	101	300	70	9.0	20.0

Ultrahigh-purity hydrogen (99.999%) was used on the anode side of the fuel cell. Hydrogen was stored in a high-pressure tank, regulated to the pressure required by the experiment, and its flow rate measured by a mass flow meter. Because of the dead-end anode design of the fuel cell, hydrogen mass flow rate was not controlled, only monitored.

The external electrical circuit consisted of a bank of light-emitting diode (LED) lights whose resistance varied with applied voltage, which was measured for each experimental voltage.

Data were collected and logged in real-time via National Instruments data acquisition (DAQ) hardware (DAQPad 6020E) and Labview software interface. Instrumentation used in the experiment along with associated maximum uncertainty is listed in Table 1.

Table 2 gives a summary of the range of controlled variables for the results presented in this paper. The conditions represented by these pressure and temperature conditions range from sea level to 53,500 feet (16,307 m) in altitude. The statistical method of design of experiments (DOEx) was used to assign the values of each variable (factor) to each randomized test run, which enables an analysis of variance (ANOVA) approach to data analysis. The result of using this method is not only a greatly reduced experimental set compared to traditional one-factor-at-a-time (OFAT) methods, but also an ability to identify how interactions between variables affect the results, determine whether observations are statistically significant when compared to experimental error, and provide measures of uncertainty for the data set including interpolated and extrapolated performance values. This approach has been used before in fuel cell experiments as in [20].

Results and Discussion

The raw data collected are shown in Table 3. They are presented for completeness and to provide results that can be used by others in computer model development or design for altitude operation of a PEMFC system. Because these data were collected in accordance with the guidelines of DOEx, they are designed to be examined using ANOVA significance analysis with results shown in Figs. 1 and 2.

Although experiments were conducted under conditions that simulate altitudes up to approximately 53,500 feet (16,307 m) (Runs 29, 30, 33, 34, 35, and 37) there were not enough data collected at these very low-pressure conditions to allow extending the ANOVA analysis to this altitude. This was partially due to experimental limitations that did not allow for high-flow, low-pressure testing, which eliminated some experiments from the test matrix. Analyzing an incomplete test matrix with the ANOVA technique can produce unreliable results, so these data were not included in the ANOVA analyses.

Note that responses of stack current and voltage, hydrogen flow, and hydrogen pressure are presented as a function of the controlled variables.

Figure 1 presents the results of the experiment in the form of voltage-current ($V-i$) curves. These curves were generated by the ANOVA analysis of the experimental data and are given for the combination of pressures and airflow rates shown in the figure. The curves are valid for the entire range of relative humidity (15–70% RH) and air inlet temperature (−60 to +20°C) because the effects of air inlet temperature and humidity were measured to be statistically insignificant in the ranges studied. The shape of the $V-i$ curves indicates that the fuel cell was operating in the transition region between the low- and middle-current regimes, where activation and ohmic losses dominate.

Clearly, lower total pressure leads to a downward shift in the $V-i$ curve toward lower voltage performance and an increase in the slope of the curve, regardless of the airflow rate. Another observation is that the effect of airflow at low pressures is greater than the effect at higher pressures.

To understand the reasons behind these observations it is necessary to look at the fuel cell governing principals and physical characteristics, beginning with the Nernst equation [Eq. (2)].

One phenomenon of the Nernst equation when applied to the PEMFC is that the Nernst voltage increases when total cathode pressure is lowered and all other variables are held constant. To see this, the substitution of Eq. (1) into Eq. (2) along with distinguishing between the total pressure of the anode and the cathode gives

$$E = E^\circ + \frac{RT}{nF} \ell_n \frac{x H_2 P_A (x O_2 P_C)^{\frac{1}{2}}}{x H_2 O P_C} \qquad (3)$$

Isolating the relationship between Nernst voltage and total cathode pressure gives

$$E \propto - \ell_n (P_C) \qquad (4)$$

Obviously the $V-i$ curves in Fig. 1 show the opposite effect, that of decreasing voltage when cathode pressure is lowered. This is because in addition to the effects on the Nernst equation, oxygen concentration and total pressure adversely affected fuel cell performance to a much greater degree through the irreversible losses (activation, ohmic, and mass diffusion) that all operating fuel cells experience.

Activation Loss

Activation loss is associated with the reaction kinetics and the fact that some charge buildup must occur at the electrode reaction site to drive the reaction forward. The energy required to activate the charge transfer process at the reaction site is lost and does not contribute to the realized voltage. This loss is most obvious at low-current densities, when the amount of charge building up is a large fraction of the total charge associated with the overall reaction.

Application of transition state theory to the electron transfer process of an electrochemical reaction results in the well-known Butler–Volmer expression that describes activation polarization [32]:

Table 3   Experimental data

Run no.	Controlled variables					Measured responses			
	Chamber (cathode) pressure, kPa (absolute)	External resistance, Ω	Air inlet relative humidity, %	Airflow, SLPM	Air inlet temperature, °C	Stack voltage, VDC	Stack current, A	Hydrogen flow, SLPM	Hydrogen (anode) pressure, kPa (absolute)
1	44.46	38.93	38.52	4.99	4.82	11.08	0.37	0.080	148.25
2	83.96	74.49	61.10	1.00	13.10	15.19	0.22	0.058	187.54
3	24.72	89.08	15.45	9.00	15.06	12.54	0.15	0.042	127.36
4	83.75	21.12	15.14	9.01	−5.47	12.15	0.72	0.150	187.27
5	84.14	21.40	59.85	9.00	14.94	12.05	0.72	0.150	187.49
6	24.68	82.58	60.60	8.95	−4.87	13.67	0.18	0.048	127.95
7	84.04	22.88	59.43	1.00	−19.87	11.51	0.64	0.135	186.92
8	24.89	46.11	36.99	5.00	−9.89	9.79	0.27	0.059	127.66
9	24.47	46.02	37.44	5.03	−9.92	9.80	0.27	0.060	127.53
10	83.85	20.09	60.29	8.91	−0.23	12.56	0.76	0.160	188.08
11	84.13	22.98	14.34	1.00	−0.29	11.47	0.64	0.137	187.23
12	83.97	72.47	14.38	0.99	−4.38	15.95	0.24	0.064	187.25
13	83.88	72.04	58.90	1.00	−0.19	16.11	0.25	0.065	186.25
14	83.92	72.06	14.61	8.98	−0.12	16.11	0.24	0.064	187.50
15	84.23	20.02	15.18	9.00	−19.86	12.61	0.75	0.159	187.97
16	84.04	71.98	14.83	1.02	−20.01	16.14	0.24	0.064	187.74
17	84.32	71.83	56.66	9.00	−19.67	16.19	0.24	0.065	186.32
18	84.01	72.57	27.31	1.02	−57.54	15.91	0.24	0.065	186.71
19	24.49	36.35	36.79	9.48	−29.89	11.68	039	0.088	127.26
20	84.02	19.50	58.55	9.00	−19.85	13.03	0.81	0.168	186.93
21	24.53	38.05	36.39	4.94	−40.01	11.28	0.37	0.083	128.14
22	84.10	19.29	30.53	9.00	−60.16	13.20	0.82	0.171	187.33
23	83.97	71.37	59.33	1.02	−18.94	16.37	0.25	0.066	188.10
24	101.65	70.97	64.68	9.00	20.19	16.52	0.25	0.067	204.13
25	101.68	29.14	63.11	5.18	20.29	14.33	0.57	0.128	203.77
26	101.89	19.87	68.16	8.81	20.41	12.73	0.77	0.164	206.26
27	101.97	71.82	62.90	1.00	22.57	16.20	0.24	0.066	206.48
28	101.91	29.32	67.34	5.01	23.41	14.25	0.58	0.127	203.54
29	9.90	102.82	29.11	3.24	−60.05	11.03	0.11	0.034	112.66
30	15.78	100.51	24.97	2.11	−29.88	11.28	0.12	0.037	119.02
31	24.36	80.99	19.41	3.23	−59.97	13.95	0.19	0.052	127.88
32	24.55	85.37	25.76	1.01	−0.34	13.19	0.17	0.048	128.38
33	15.54	98.97	22.16	2.12	−28.82	11.45	0.13	0.038	119.19
34	10.01	276.52	24.74	0.97	0.03	6.71	0.03	0.011	113.86
35	9.96	182.00	23.55	3.20	0.25	7.70	0.05	0.015	113.36
36	24.56	85.40	25.15	3.22	−0.21	13.18	0.17	0.048	127.49
37	10.06	117.06	26.82	1.01	−56.55	9.74	0.08	0.026	113.90
38	25.38	84.07	46.00	0.96	−60.31	13.41	0.17	0.049	127.14
39	102.39	21.60	61.41	0.92	21.85	11.98	0.68	0.147	206.22
40	24.42	54.09	38.62	4.97	−40.33	9.17	0.25	0.058	126.57
41	101.20	30.43	57.68	4.94	21.89	13.70	0.57	0.131	204.91
42	84.01	77.19	13.31	0.97	−19.04	14.62	0.22	0.063	186.04
43	26.16	99.62	17.69	1.04	−0.43	11.38	0.14	0.043	127.65
44	83.92	74.11	60.51	9.00	−19.85	15.34	0.24	0.066	188.02
45	83.43	21.92	12.72	8.92	−20.34	11.86	0.71	0.154	186.66
46	101.68	74.86	52.60	0.98	19.44	15.05	0.22	0.063	204.68

$$i = i_o \left\{ \exp\left[-\alpha \frac{FV_{\text{act}}}{RT} \right] - \exp\left[(1-\alpha) \frac{FV_{\text{act}}}{RT} \right] \right\} \qquad (5)$$

The exchange current can be thought of as the "idle" current at the electrode, that is, the totally reversible equilibrium current of a particular reaction (with no net current flow) [32]. For the oxygen reduction reaction (ORR) at the PEMFC cathode equilibrium is established in the following reaction:

$$\tfrac{1}{2}O_2 + 2H^+ + 2e^- \Leftrightarrow H_2O \qquad (6)$$
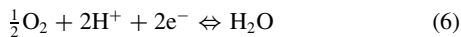
producing an idle current corresponding to oxygen being reduced to water at exactly the same rate that it is being produced. The rate of this exchange between O_2 and H_2O is given by the exchange current. If the current demanded out of the fuel cell is less than the exchange current, the current is readily supplied. However, if the current required exceeds the exchange current, an equilibrium "shift" must be made and this is manifested by a much larger voltage loss.
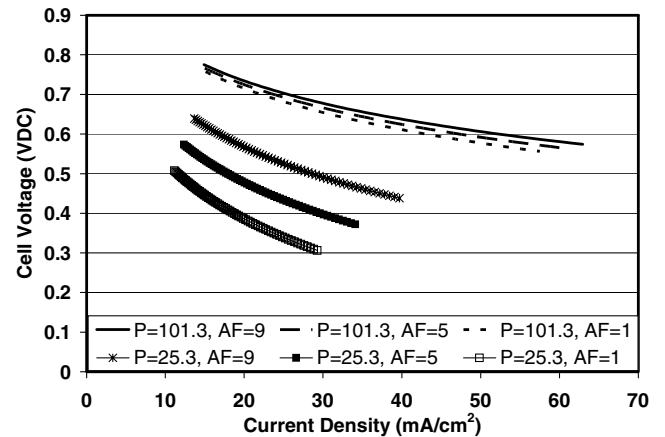
Fig. 1   **Effect of pressure and airflow rate on cell performance as given by ANOVA analysis of experimental results, 95% confidence level. Pressure (P) given in kPa (absolute) and airflow (AF) given in SLPM.**
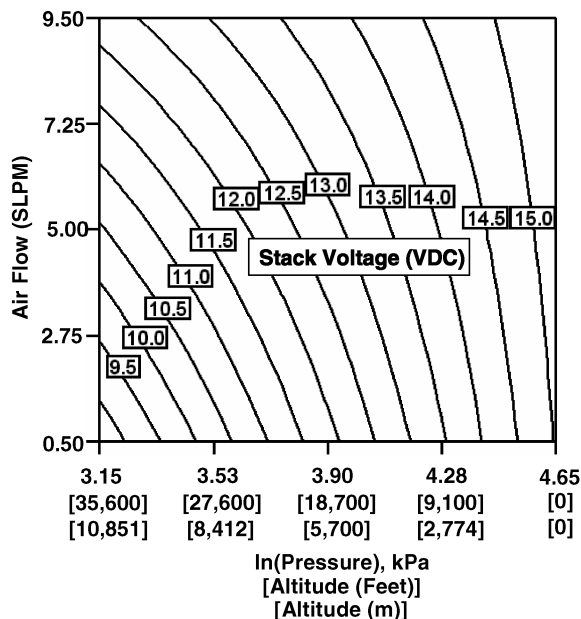
Fig. 2 Interaction of ambient pressure and airflow and their effects on stack voltage for a fixed external resistance (50 Ω).

Fig. 3 Standard error (in VDC) associated with the results shown in Fig. 2.

Therefore, an electrode with a large exchange current will have a smaller voltage loss than one with a small exchange current.

Exchange current can be expressed in several ways [32–35], for simplicity and without sacrificing the pertinent details, the equation

$$i_o = nFk(pO_2)^y \frac{1000}{A_{\text{cell}}} \qquad (7)$$

is assumed. Equation (7) is based on [33] which considers only the ORR at the cathode, and with the concentration of oxygen being replaced by the oxygen partial pressure (pO_2), which is more appropriate in the case of a gas-fed fuel cell because total pressure can now be considered as a factor as well. n is the number of electrons participating in the reaction of the rate determining step, k is the electrochemical rate constant, and y is the reaction order with respect to oxygen partial pressure ($y = 1$ is assumed in most analyses, e.g., [33]). A_{cell} is the cell area (cm^2), so by assuming partial pressure is normalized to 1 bar, the units work out to mA/cm^2. Thus exchange current, and as a result activation loss, is a function of both oxygen concentration and total pressure via the oxygen partial pressure term of Eq. (7). As either concentration or total pressure increases, so does the exchange current, resulting in a overall decrease in activation loss.

In this experiment, oxygen concentration was not varied directly; however, Kulikovsky [23] shows that airflow is connected to oxygen concentration through the stoichiometric ratio λ. As airflow, and thus λ, is decreased, the oxygen concentration goes down. This reference also indicated that a λ > 3 did not result in a large concentration change across the cell, which for a fuel cell operating in the low-current regime led to a hardly noticeable change in cell potential. The experiment of the present work had stoichiometric ratios of λ ≅ 3 for the 0.5 standard liter per minute (SLPM) case and λ ≅ 60 for the 9.5 SLPM case. Thus, one can assume that the oxygen concentration did not vary by an appreciable amount except in the very low airflow cases. Of course oxygen concentration can vary due to other factors such as cathode water content. However, in this experiment airflow is the most direct indicator of oxygen concentration because variations in water content of the inlet stream, water generated by the fuel cell, and oxygen consumed by the fuel cell, were measured to contribute a maximum of a 3.1% change in oxygen concentration across all experiments.

In Fig. 1 the downward shift of V–i curves as pressure or airflow is lowered is characteristic of increasing activation loss, and is expected from the theoretical point of view. Examination of Fig. 1 also shows
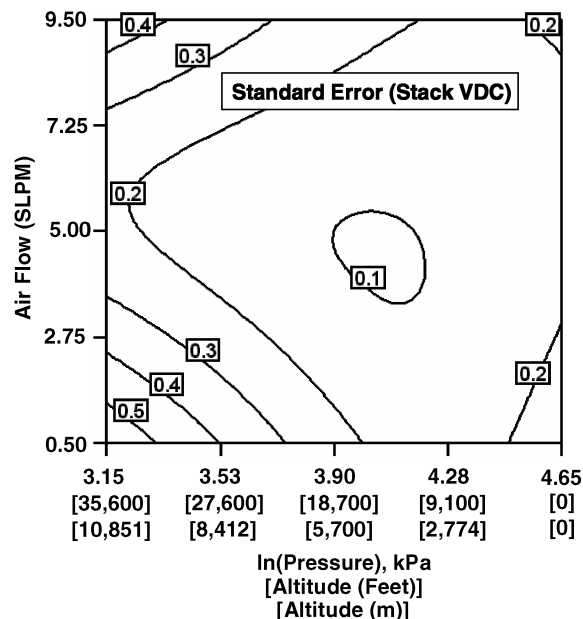
an interaction between total pressure and airflow, where airflow has little effect at high pressure but a large effect at low pressure. This can be seen in the ANOVA interaction contour graph, Fig. 2, which is also valid for the entire range of relative humidity (15–70% RH) and air inlet temperature (−60 to +20°C) for the same reasons as described in the preceding section. The figure is plotted for a given external resistance, in this case 50 Ω is chosen, although other external resistance will have similar behavior.

(Notice that in the ANOVA graph individual data points are not shown because an ANOVA-designed experiment produces an entire response surface with best-fit interpolation between actual data points, and the areas of interest shown in Fig. 2 do not necessarily correspond to exactly one or more data points. For more detail on the DOEx and ANOVA process the reader can refer to one of several texts on the subject [36], or an illustrative example [37].)

Figure 2 shows a key interaction, that between pressure and airflow. For both the high- and low-airflow cases, the voltage decreases with a decrease in pressure. In this graph it is easy to see that at low pressure the effect of a decrease in airflow is significant. At high pressure, and using the standard error for this condition as shown in Fig. 3, it can be seen that the effect of airflow at this condition is negligible (within experimental error).

Figure 3 shows the standard error [in volts, direct current (VDC)] of the experimental results of Fig. 2. In comparing these two figures it can be seen that the spacing between adjacent voltage contours of Fig. 2 is sufficient to distinguish real differences in experimental results in all areas except the extreme upper left and lower left corners. Also it is easy to see that at the high-pressure condition [$\ell_n(P) = 4.65$] the change in voltage with a change in airflow is within the standard error of the experiment.

According to the preceding discussion and Eqs. (5) and (7), equal changes in total pressure or concentration should affect the voltage loss equally. As a starting point for comparison, consider the case of ambient pressure [$\ell_n(P) = 4.65$] and negligible concentration change (airflow of 9.50 SLPM). The stack voltage at this point is 15.4 VDC. If we use the numbers from [23], a λ = 3 case would lead to an oxygen concentration decrease of approximately 33% (xO_2, exit/xO_2, inlet), which if $P_T = 1$, would lead to a partial pressure decrease of 33% according to Eq. (1). This corresponds to the 0.50 SLPM and $\ell_n(P) = 4.65$ case where the stack voltage is 15.0 VDC, or a 0.017 V/cell decrease in cell voltage. The same decrease in partial pressure accomplished by varying total pressure instead (keeping concentration constant) would correspond to a pressure of 70 kPa ($\ell_n(P) = 4.25$). For this case, the stack voltage would

decrease to 14.6 VDC, or 0.35 V/cell. Although within experimental uncertainties, this result confirms observations of previous research [13,15–18] suggesting a greater dependence of voltage on total pressure than oxygen partial pressure, and there must be another mechanism responsible for the imbalance.

(It would be interesting and very useful to see if the analytical expressions developed by Kulikovsky [23] could be modified to include the effects of pressure and solved. However, Kulikovsky points out that it is not likely that an analytical solution for the required system of equations would be found.)

Ohmic Loss

The irreversibilities of the ionic and electronic conduction processes are considered through ohmic losses. Ohmic loss is calculated by combining ionic and electronic resistances in the fuel cell and interconnecting components into a parameter of overall resistance, R_{cell}. This resistance contributes to the $V–i$ curve's characteristic linear negative slope. It is assumed that R_{cell} in this experiment has negligible dependence on concentration or total pressure (for example, Buchi and Scherer [38] show a change in resistance of Nafion 117 of less than 5% when total pressure was increased three times). R_{cell} could also be influenced by cell temperature and reactant humidity, but in these experiments the effects of air inlet temperature and humidity were measured to be statistically insignificant in the ranges studied. This unexpected observation is most likely due to the low-current density operation and design of the stack and experimental setup, in addition to the fact that the relative humidity changes were done on the cathode side of the stack and not the anode side. Thus we look to the third loss mechanism for an explanation of the unbalanced effects of concentration and pressure on the $V–i$ curve.

Diffusion Loss

Mass diffusion loss is associated with the nonideal mass transport of gases to and from the electrochemical reaction site. To understand this mechanism and the difference between the effects of oxygen concentration and total pressure, it is necessary to look into the structure of the fuel cell cathode and consider the chemical and physical processes that govern mass transport there. Many studies have described these details [9,17,21,34,39–41], so just a summary is presented here.

There are typically two layers to a cathode, a backing layer on the gas side and a catalyst layer on the electrolyte side. The primary function of the catalyst layer is to provide a site where the reactant gas can react with ions from the electrolyte and electrons from the external circuit. The primary function of the backing layer is to provide mechanical support for the fuel cell while allowing sufficient reactant and product gas diffusion through it to and from the catalyst layer. Both layers must also be electronically conductive.

Because of their different primary functions, the catalyst and backing layers have different physical characteristics. The backing layer needs to find the perfect balance between strength, porosity, and thickness. The catalyst layer needs to provide a balance between access to the electrolyte and reaction sites, containment of liquid water close to the electrolyte, and porosity.

These balances have led to the development of cathodes that have backing layers with large pores and catalyst layers with a mixture of large and small pores. The porosity is important because diffusion characteristics of gases into and out of the backing and catalyst layers have a large effect on the irreversible losses. For example, Iczkowski and Cutlip [39] show that in a phosphoric acid fuel cell the gas diffusion processes have nearly the same impact on voltage loss as all the ohmic (electronic and ionic) processes. (Ridge et al. [40] note that a PEMFC porous electrode can be modeled similar to the PAFC porous electrode model presented in [39].)

Diffusion through the large pores of the backing layer has been shown to be molecular diffusion [17,34,39], following the Stefan–Maxwell equation, and as such depends on concentration but not on total pressure [17,21,39,42].

The dependence on pressure and concentration in the catalyst layer is more complex. Diffusion through the catalyst layer is generally accepted to be at least part molecular diffusion (large pores) and part Knudsen diffusion (small pores) [34,39]. It is also theorized that grain boundary diffusion plays a role [17,34,39], and pressure and concentration also affect the dissolution of oxygen into the liquid water in the catalyst layer near the electrolyte governed by Henry's law [17]. (Note that if liquid water were to penetrate into the backing layer, Henry's law would apply to the diffusion process there, and then backing layer diffusion would also become total pressure-dependent.) Regardless of the exact contributions of each of these methods, the fact that diffusion in the catalyst layer is not entirely molecular means that total pressure also affects diffusion losses. Iczkowski and Cutlip [39] estimated that of the total gas diffusion losses, diffusion in the backing layer (molecular) accounted for 37%, molecular diffusion in the catalyst layer accounted for 26%, and Knudsen diffusion in the catalyst layer 37%. If this were generally true for current PEM technology, then 63% of diffusion losses are affected by concentration alone, and 37% are affected by total pressure alone (note that Knudsen diffusion is not affected by concentration) [21,42].

It follows that as total pressure is decreased while concentration is held constant (e.g., as with increasing altitude), the Knudsen diffusion losses will increase while molecular diffusion losses remain constant. Therefore as total pressure is reduced, Knudsen diffusion losses comprise an ever larger proportion of the total diffusion losses. This is confirmed experimentally by the observed increased importance of the catalyst layer diffusion processes as total pressure is decreased in [17].

The combined effect of all the mass diffusion mechanisms on the voltage loss of the fuel cell is to increase the downward slope of the $V–i$ curve, especially as current is increased. This trend is noticeable in Fig. 1 as each $V–i$ curve has a slightly larger downward slope than the one above it.

In the present experimental work, this imbalance between the effects of total pressure and concentration on mass diffusion loss is responsible for the discrepancy mentioned earlier between the observed loss due to total pressure and that due to concentration. Looking at the highest airflow (9.5 SLPM, where oxygen concentration can be assumed constant throughout the cell) in shows the impact of pressure alone on stack voltage: a stack voltage decrease from 15.4 to 12.2 V, or a 0.13 V/cell decrease when $\ell_n(P)$ is decreased from 4.65 to 3.15. Compared to the loss due to concentration changes described earlier of 0.017 V/cell, we can see that this experiment was dominated by losses due to total pressure changes.

An interesting observation from this experiment is that at the lowest airflow (0.5 SLPM) shown in it can be seen that when low pressure is combined with lower concentration, the voltage loss is greater than the simple sum of both cases. From the "no loss" case of $\ell_n(P) = 4.65$, airflow = 9.5 SLPM to the "worst case" of $\ell_n(P) = 3.15$, airflow = 0.5 SLPM, the voltage decreases from 15.4 to 8.6 VDC, a 0.28 V/cell decrease. This level of performance degradation is almost twice the sum of the losses due to pressure (0.13 V/cell) and concentration (0.017 V/cell) alone. This strong positive interaction between low pressure and low concentration suggests that there are other mechanisms involved that warrant further investigation.

The optimum high-altitude fuel cell would have a structure designed to facilitate mass diffusion in low total pressure operation. There are many ways this can be achieved; for example, Goodenough and Cushing [33] and Lee et al. [43] note that whereas increasing the amount of electrolyte incorporated into the catalyst layer improves proton conduction leading to better performance, it also leads to larger pores being blocked. This makes Knudsen diffusion a more prominent diffusion mechanism. For fuel cells operating at high total pressure, lower Knudsen diffusion losses could potentially decrease overall diffusion losses leading to a significant increase in performance. But fuel cells operating at low total pressure could exhibit higher Knudsen diffusion losses that

could result in a decrease in fuel cell performance (especially at high current densities).

Catalyst layer design thickness decisions become more complex when total pressure effects are taken into account. It has been shown that the primary region of operation on the $V–i$ curve [small current (activation), medium current (ohmic), and high current (O_2 depletion)] affects the optimum catalyst layer design, as does the reaction rate [34]. Low currents and low reaction rates both favor thicker catalyst layers [34], but thicker catalyst layers increase the total pressure loss thus making low total pressure operation less desirable. On the contrary, high currents and high reaction rates favor thinner catalyst layers, which is a more desirable condition for low total pressure fuel cell operation. This also shows that increasing catalyst layer thickness to compensate for low reaction rate may not be the best solution when low-pressure fuel cells are considered.

The backing layer design of the low-pressure fuel cell need not differ from its high-pressure counterpart. Because oxygen diffusion through the backing layer depends on concentration and not on total pressure (described in the preceding paragraphs), as long as the backing layer is designed for the concentration of oxygen present in air it should perform the same regardless of total pressure. This also shows why the so-called nitrogen blanketing effect, which is caused by the inert gas in the cathode stream impeding oxygen molecular diffusion through the backing layer [17,34], is unaffected by changes in total pressure.

Conclusions

Whereas the theory shows that changes in concentration affect a fuel cell differently than changes in total pressure, until now this has only been confirmed by experiments involving increasing the total pressure above 1 atm. The present research (the first known published experiment of a fuel cell operating at a significant subatmospheric pressure) confirms the applicability of this theory to fuel cell operation with total pressures below 1 atm and shows a clear decrease in performance of a proton exchange membrane fuel cell when subjected to total pressures down to 23.3 kPa. The results showed the distinction between voltage loss due to concentration effects (because of limited air stoichiometry) and those due to total pressure effects where it was shown that between equal percentage decreases of concentration and total pressure, total pressure had a greater effect on performance.

When both concentration and total pressure were reduced, the measured voltage loss exceeded the sum of the observed voltage losses from the separate cases. This observation suggests a possible compounding effect that deserves further investigation.

The current data set provides the magnitude of decrease in fuel cell performance with high-altitude operation for a specific PEMFC. Together with the theoretical information and discussion provided, it is hoped that designers of aeronautical fuel cell systems will be aided in determining optimum physical characteristics and design operating conditions.

Acknowledgment

References

[1] Freeh, J. E., Pratt, J. W., and Brouwer, J., "Development of a Solid-Oxide Fuel Cell/Gas Turbine Hybrid System Model for Aerospace Applications," ASME Paper GT2004-53616, 2004.

[2] Daggett, D., Freeh, J., Balan, C., and Birmingham, D., "Fuel Cell APU for Commercial Aircraft," *2003 Fuel Cell Seminar Abstracts*, Miami Beach, FL, Nov. 2003.

[3] Knaupp, W., and Mundschau, E., "Solar Electric Energy Supply at High Altitude," *Aerospace Science and Technology*, Vol. 8, No. 3, 2004, pp. 245–254.

[4] Dornheim, M., "Special Fuel Cells Key To Months-Long Flight: Having Mastered Solar-Powered Flight, AeroVironment's Final Step is to Efficiently Store Energy for Nighttime Use," *Aviation Week and Space Technology*, Vol. 152, No. 9, 2000, pp. 58–61.

[5] Anon., "Boeing Receives Contract for UAV Advanced Propulsion System," *Boeing News Release*, 2002, http://www.boeing.com/news/releases/2002/q3/nr_020903m.html [cited Sept. 2006].

[6] Anon., "World News Roundup," *Aviation Week & Space Technology*, Vol. 157, No. 11, Sept. 2002, pp. 26–27.

[7] "GenCore Systems, Fuel Cell Products for Premium Power Generation," Plug Power, Inc., Latham, NY, 2003.

[8] United States Committee on Extension to the Standard Atmosphere, *U. S. Standard Atmosphere, 1976*, U.S. Government Printing Office, Washington, DC, 1976, p. 9.

[9] Larminie, J., and Dicks, A., *Fuel Cell Systems Explained*, John Wiley & Sons, West Sussex, England, 2000.

[10] EG&G Services, Parsons, Inc., and Science Applications International Corporation, *Fuel Cell Handbook*, 5th ed., U.S. Department of Energy, Morgantown, WV, 2000.

[11] Ticianelli, E. A., and Gonzalez, E. R., "Fundamental Kinetics/Transport Processes in MEAs," *Handbook of Fuel Cells, Fundamental Technology and Applications, Volume 2 Electrocatalysis*, edited by W. Vielstich, A. Lamm, and H. A. Gasteiger, John Wiley & Sons, West Sussex, England, 2003, pp. 490–501.

[12] Srinivasan, S., Ticianelli, E. A., Derouin, C. R., and Redondo, A., "Advances in Solid Polymer Electrolyte Fuel Cell Technology With Low Platinum Loading Electrodes," *Journal of Power Sources*, Vol. 22, Nos. 3–4, 1988, pp. 359–375.

[13] Ticianelli, E. A., Derouin, C. R., and Srinivasan, S., "Localization of Platinum in Low Catalyst Loading Electrodes to Attain High Power Densities in SPE Fuel Cells," *Journal of Electroanalytical Chemistry*, Vol. 251, No. 2, 1988, pp. 275–295.

[14] Ticianelli, E. A., Derouin, C. R., Redondo, A., and Srinivasan, S., "Methods to Advance Technology of Proton Exchange Membrane Fuel Cells," *Journal of the Electrochemical Society*, Vol. 135, No. 9, 1988, pp. 2209–2214.

[15] Srinivasan, S., Velev, O. A., Parthasarathy, A., Manko, D. J., and Appleby, A. J., "High Energy Efficiency and High Power Density Proton Exchange Membrane Fuel Cells—Electrode Kinetics and Mass Transport," *Journal of Power Sources*, Vol. 36, No. 3, 1991, pp. 299–320.

[16] Wilson, M. S., and Gottesfeld, S., "High Performance Catalyzed Membranes of Ultra-Low Pt Loadings for Polymer Electrolyte Fuel Cells," *Journal of the Electrochemical Society*, Vol. 139, No. 2, 1992, pp. L28–L30.

[17] Springer, T. E., Wilson, M. S., and Gottesfeld, S., "Modeling and Experimental Diagnostics in Polymer Electrolyte Fuel Cells," *Journal of the Electrochemical Society*, Vol. 140, No. 12, 1993, pp. 3513–3526.

[18] Rho, Y. W., Velev, O. A., Srinivasan, S., and Kho, Y. T., "Mass Transport Phenomena in Proton Exchange Membrane Fuel Cells Using O2/He, O2/Ar, and O2/N2 Mixtures, I. Experimental Analysis," *Journal of the Electrochemical Society*, Vol. 141, No. 8, 1994, pp. 2084–2089.

[19] Paganin, V. A., Ticianelli, E. A., and Gonzalez, E. R., "Development of Electrochemical Studies of Gas Diffusion Electrodes for Polymer Electrolyte Fuel Cells," *Journal of Applied Electrochemistry*, Vol. 26, No. 3, 1996, pp. 297–304.

[20] Amphlett, J. C., Baumert, R. M., Mann, R. F., Peppley, B. A., and Roberge, P. R., "Performance Modeling of the Ballard Mark IV Solid Polymer Electrolyte Fuel Cell, 1. Mechanistic Model Development," *Journal of the Electrochemical Society*, Vol. 142, No. 1, 1995, pp. 1–8.

[21] Kocha, S. S., "Principles of MEA Preparation," *Handbook of Fuel Cells, Fundamental Technology and Applications, Volume 3 Fuel Cell Technology and Applications Part 1*, edited by W. Vielstich, A. Lamm, and H. A. Gasteiger, John Wiley & Sons, West Sussex, England, 2003, pp. 538–565.

[22] Prasanna, M., Ha, H. Y., Cho, E. A., Hong, S.-A., and Oh, I.-H., "Investigation of Oxygen Gain in Polymer Electrolyte Membrane Fuel Cells," *Journal of Power Sources*, Vol. 137, No. 1, 2004, pp. 1–8.

[23] Kulikovsky, A. A., "The Effect of Stoichiometric Ratio λ on the Performance of a Polymer Electrolyte Fuel Cell," *Electrochimica Acta*, Vol. 49, No. 4, 2004, pp. 617–625.

[24] Atkins, P., *Physical Chemistry*, 5th ed., W. H. Freeman and Company, New York, 1994, pp. 866–868.

[25] Josefik, N. M., Binder, M. J., Taylor, W. R., and Holcomb, F. H., "The Department of Defense Fuel Cell Demonstration Program," *2002 Fuel Cell Seminar Abstracts*, Palm Springs, CA, Nov. 2002.

[26] Evans, M., "Powering up at Yellowstone—Entrance Station Using Innovative Fuel Cell to Meet Electricity Demand," *Post Register*, Post Company, Idaho Falls, ID, Aug. 2002.

[27] Chang, V., and Gallman, J., "Altitude Testing of Fuel Cell Systems for Aircraft Applications," SAE Paper 2004-01-3200, 2004.

[28] Spiegel, R. J., Gilchrist, T., and House, D. E., "Fuel Cell Bus Operation at High Altitude," *Proceedings of the Institution of Mechanical Engineers, Part A, Journal of Power and Energy*, Vol. 213, No. 1, 1999, pp. 57–68.

[29] Wilson, M. S., "Annular Feed Air Breathing Fuel Cell Stack," United States Patent 5,514,486, 1996.

[30] Wexler, A., "Vapor Pressure Formulation for Water in Range 0 to 100°C. A Revision," *Journal of Research of the National Bureau of Standards. Section A. Physics and Chemistry*, Vol. 80A, Nos. 5, 6, 1976, pp. 775–785.

[31] Wexler, A., "Vapor Pressure Formulation for Ice," *Journal of Research of the National Bureau of Standards. Section A. Physics and Chemistry*, Vol. 81A, No. 1, 1977, pp. 5–20.

[32] Bard, A. J., and Faulkner, L. R., *Electrochemical Methods Fundamentals and Applications*, 2nd ed., John Wiley & Sons, Hoboken, NJ, 2001, pp. 98–107.

[33] Goodenough, J. B., and Cushing, B. L., "Oxide-Based ORR Catalysts," *Handbook of Fuel Cells, Fundamental Technology and Applications, Volume 2 Electrocatalysis*, edited by W. Vielstich, A. Lamm, and H. A. Gasteiger, John Wiley & Sons, West Sussex, England, 2003, pp. 520–533.

[34] Eikerling, M., and Kornyshev, A. A., "Modelling the Performance of the Cathode Catalyst Layer of Polymer Electrolyte Fuel Cells," *Journal of Electroanalytical Chemistry*, Vol. 453, Nos. 1–2, 1998, pp. 89–106.

[35] Ota, K., and Mitsushima, S., "O2 Reduction on the Pt/Polymer-electrolyte Interface," *Handbook of Fuel Cells, Fundamental Technology and Applications, Volume 2 Electrocatalysis*, edited by W. Vielstich, A. Lamm, and H. A. Gasteiger, John Wiley & Sons, West Sussex, England, 2003, pp. 481–489.

[36] Mason, R. L., Gunst, R. F., and Hess, J. L., *Statistical Design and Analysis of Experiments With Applications to Engineering and Science*, 2nd ed., John Wiley & Sons, Hoboken, NJ, 2003.

[37] Simpson, J. R., and Wisnowski, J. W., "Streamlining Flight Test with the Design and Analysis of Experiments," *Journal of Aircraft*, Vol. 38, No. 6, 2001, pp. 1110–1116.

[38] Buchi, F. N., and Scherer, G. G., "In-situ resistance measurements of Nafion® 117 membranes in polymer electrolyte fuel cells," *Journal of Electroanalytical Chemistry*, Vol. 404, 1996, pp. 37–43.

[39] Iczkowski, R. P., and Cutlip, M. B., "Voltage Losses in Fuel Cell Cathodes," *Journal of the Electrochemical Society*, Vol. 127, No. 7, 1980, pp. 1433–1440.

[40] Ridge, S. J., White, R. E., Tsou, Y., Beaver, R. N., and Eisman, G. A., "Oxygen Reduction in a Proton Exchange Membrane Test Cell," *Journal of the Electrochemical Society*, Vol. 136, No. 7, 1989, pp. 1902–1909.

[41] Mathias, M. F., Roth, J., Fleming, J., and Lehnert, W., "Diffusion Media Materials and Characterisation," *Handbook of Fuel Cells, Fundamental Technology and Applications, Volume 3 Fuel Cell Technology and Applications Part 1*, edited by W. Vielstich, A. Lamm, and H. A. Gasteiger, John Wiley & Sons, West Sussex, England, 2003, pp. 517–537.

[42] Bird, R. B., Stewart, W. E., and Lightfoot, E. N., *Transport Phenomena*, 2nd ed., John Wiley & Sons, New York, NY, 2002, pp. 793–798.

[43] Lee, S. J., Mukerjee, S., McBreen, J., Rho, Y. W., Kho, Y. T., and Lee, T. H., "Effects of Nafion Impregnation of Performances of PEMFC Electrodes," *Electrochimica Acta*, Vol. 43, No. 24, 1998, pp. 3693–3701.

C. Avedisian
Associate Editor